Tellus (2004), 56B, 339–356
Printed in UK. All rights reserved

TELLUS

Radon global simulations with the multiscale chemistry and transport model MOCAGE

By B. JOSSE*, P. SIMON and V.-H. PEUCH, *Météo-France, Centre National de Recherches Météorologiques, 42 av G. Coriolis, 31057 Toulouse, France*

(Manuscript received 29 July 2003; in final form 16 March 2004)

ABSTRACT

We present an evaluation of the representation of subgrid scale transport in the new multiscale global chemistry and transport model MOCAGE. The approach is an off-line computation of vertical mass fluxes due to convective and turbulent processes, using only large-scale variables archived in meteorological analyses. Radon is a naturally emitted gas with a radioactive half-life of 3.8 days and is a useful tracer of tropospheric transport processes. A 1-yr (1999) simulation of atmospheric radon concentration has been performed, using 6-hourly meteorological analyses for the forcings. Two different mass flux convection schemes have been tested: a simplified version of the Tiedtke (1989) scheme and Kain–Fritsch–Bechtold (Bechtold et al., 2001). We compare model outputs with observations at different time and space scales, showing good overall results. A new interpretation is given to the more contrasted results obtained in Antarctica, as for other models. The state-of-the-art representation of synoptic scale activity around Antarctica is markedly worse than in other parts of the world, both due to oversimplifications of the seasonal evolution of the extent of sea ice, and to the scarcity of observations. Twelve-hourly simulated concentrations are evaluated at two sites for 1999. At Amsterdam Island results are satisfactory: correlation between observed and modelled concentrations is of the order of 0.5. The model reproduces well "radonic storm" events. At the coastal site of Mace Head in Ireland, simulations are available at two different horizontal resolutions. The correlation between observations and the model is of the order of 0.7. This result is mainly determined by the synoptic scale context, even though local-scale circulations such as breezes interfere on occasions. Finally, it appears that the off-line approach in MOCAGE for subgrid transport is a practical one for chemistry and transport multiscale modelling.

1. Introduction

The question of the environmental impact of human activities has received sustained attention over the last decades. In particular, increased levels of free troposphere background concentrations of ozone, precursors and aerosols, are identified as major sources of uncertainty in the radiative budget of the Earth system (IPCC, 2001). However, routine measurements of atmospheric chemistry are generally performed at the surface, with some noticeable exceptions (for instance MOZAIC, Marenco et al., 1998). Space-borne instruments, such as TERRA/MOPITT (http://www.eos.ucar.edu/mopitt/) or ENVISAT/SCIAMACHY (http://www.esa.int/envisat), capable of measuring tropospheric columns or profiles, are only now emerging and are starting to bring data on free troposphere distributions of chemical compounds of environmental interest, including ozone, carbon monoxide, methane and nitrogen oxides.

This situation has two consequences: firstly, our understanding of the chemical composition of the free troposphere relies to a large extent on chemistry and transport model (CTM) simulations; secondly, the evaluation of these models is often limited to comparisons with surface observations, which are often poorly correlated with atmospheric concentrations, or with academic exercises, e.g. transport of passive tracers, experiments on the age of air masses and chemistry box models. In addition, tropospheric CTM evaluation is a complex task because separate measurements for sources and sinks are generally not feasible, and model biases can average out while providing satisfactory overall agreement with observations. This point advocates for separate evaluation of the different components of models, namely transport (at resolved and subgrid scales), rain-out and scavenging, chemistry (homogeneous and heterogeneous), dry deposition at the surface, and emissions. With regard to transport, ^{222}Rn simulations have been extensively used as a direct and convenient way to evaluate models (e.g. Brost and Chatfield, 1989; Jacob and Prather, 1990; Feichter and Crutzen, 1990; Genthon and Armengaud, 1995; Allen et al., 1996; Jacob et al., 1997; Stockwell and Chipperfield, 1999; Dentener et al., 1999; Chevillard

*Corresponding author.
e-mail: beatrice.josse@meteo.fr

et al., 2002). ^{222}Rn presents the interesting property of being rather uniformly emitted by non-frozen land surfaces and to have only one sink—a radioactive decay with a half-life of 3.8 days, a time scale which is comparable with that of vertical transport up to the upper troposphere. Model performances can be evaluated by comparison with surface observations over the globe and with observed vertical profiles or climatologies; model intercomparisons are also meaningful (Jacob et al., 1997), though all models may simultaneously miss some features, such as the ^{222}Rn levels at altitude over Hawaii or the shape of the annual cycle at the surface over Antarctica.

This paper presents an evaluation of transport in a new CTM, called MOCAGE (Model Of atmospheric Chemistry At larGE scale). A short account of general model characteristics is given in Section 2, together with a description of the physical parametrizations. Section 3 presents climatological results, and in Section 4 1 yr (1999) model integrations are compared with daily observations.

2. Description of model and experiments

2.1. General characteristics

MOCAGE is a semi-off-line three-dimensional CTM recently developed at Météo-France considering both the troposphere and stratosphere, on the basis of the stratospheric REPROBUS CTM (Lefèvre et al., 1994). In particular, it has been developed as a prototype for routine "chemical weather" forecasts and chemical data assimilation (Cathala et al., 2003), using validated and computationally efficient parametrizations for the relevant processes. MOCAGE dynamics are driven by meteorological analyses and, the main model domain being global, it provides its own consistent boundary conditions for chemical distribution. The meteorological analyses and short-term forecasts used in the present study come from Météo-France's operational global model, ARPEGE. ARPEGE is a version of the IFS model (http://www.ecmwf.int/research/ifsdocs); its horizontal grid is stretched and centred on France.

MOCAGE offers the interesting possibility of zooming from the global scale down to the regional one. The horizontal resolution over the globe is $2^\circ \times 2^\circ$, and up to three levels of imbricated subdomains can be simultaneously considered (Dufour et al., 2003); resolutions down to 10 km allow regional air quality modelling, forecasts and comparisons with field campaigns (Cros et al., 2004). The model comprises 47 levels on the vertical and extends up to 5 hPa; seven levels are within the planetary boundary layer (PBL), 20 are in the free troposphere and 20 in the stratosphere. The vertical coordinate is hybrid (σ, P); the first layer is 40 m thick, while the resolution above 300 hPa is constant in altitude, around 800 m. In the PBL and free troposphere the vertical levels correspond to ARPEGE, which allows interpolations for the forcing data and subsequent numerical problems to be avoided. For the present study, 6-hourly temperature, pressure, specific humidity and horizontal wind are used. A semi-Lagrangian scheme is used for advection of tracers and chemical compounds; it is based upon the work of Williamson and Rasch (1989) and has been extensively used in an earlier stratospheric version of the model (Lefèvre et al., 1994; WMO, 1998). A simple correction scheme is applied in order to ensure total mass conservation during transport. Time steps are 1 h for advection and 15 min for subgrid-scale processes, described in the next section, as well as for source and sink processes.

2.2. Physical subgrid parametrizations

Transport by diffusive and convective processes is an important component of the transport model. As mass exchange fluxes are generally not available (especially for instance when using meteorological analyses), it is worthwhile addressing the question of diagnosing these fluxes starting from the large-scale variables only.

2.2.1. Turbulent diffusion. Turbulent mixing is treated in the model following Louis (1979), as in ARPEGE. Horizontal diffusion is neglected, while the vertical diffusion coefficient K depends on height, wind shear and atmospheric stability:

$$K = l^2 \left| \frac{\Delta v}{\Delta z} \right| F(Ri)$$

where l is mixing length, v the wind module, Ri is the Richardson number and F is a function decreasing with Ri. The more unstable the atmosphere, the greater K.

2.2.2. The Tiedtke scheme for convection. Two convection schemes are alternatively used for the present study; both are of a mass-flux type. The first one is a simplified version of that of Tiedtke (1989): downdrafts, inside-cloud subsidence, as well as organized entrainment over cloud base are neglected. Downdraft mass fluxes have been estimated to be one-tenth of updraft mass fluxes and are also neglected in some other CTMs (e.g. Collins et al., 2002). Penetrative convection is assumed to occur when both a deep layer of conditional instability and a large-scale moisture convergence exist. This dependence on moisture convergence implies an influence of the columns surrounding the column we consider. For shallow convection, moisture balance is still imposed, but in this case the contribution of moisture convergence becomes smaller or even negligible, and surface evaporation is largely responsible for convection.

Tiedtke's scheme is based on the computation of mass fluxes at each level of the convective column. The mass flux at the cloud base is computed by maintaining the moisture content in the subcloud layer. Updraft mass flux on the convective column is computed as follows:

$$\frac{\partial M_u}{\partial z} = E_u - D_u$$

where E_u (respectively D_u) is the rate of mass entrainment (respectively detrainment) per unit length. As organized entrainment is neglected, E_u amounts to turbulent entrainment

so that

$$E_u = \epsilon_u M_u \quad \text{and} \quad D_u = \delta_u M_u.$$

The fractional entrainment and detrainment rates ϵ_u and δ_u are set to constants, depending only upon the type of convection:

$$\epsilon_u = \delta_u = \begin{cases} 1 \times 10^{-4}\text{m}^{-1} \text{ for penetrative convection} \\ 3 \times 10^{-4}\text{m}^{-1} \text{ for shallow convection.} \end{cases}$$

Finally, organized detrainment is taken into account in the two model levels above the diagnosed cloud top, l_{top} and $l_{\text{top}} - 1$:

$$D_u{}^{l_{\text{top}}} = (1 - \beta) M_u{}^{l_{\text{top}}}$$

$$D_u{}^{l_{\text{top}}-1} = \beta M_u{}^{l_{\text{top}}-1}.$$

The coefficient β depends upon the type of convection: it is 0 for penetrative and 0.3 for shallow convection. Moreover, environmental compensatory subsidence is taken into account to ensure mass equilibrium inside the convective column.

2.2.3. The Kain–Fritsch–Bechtold scheme for convection. This scheme, described in Bechtold et al. (2001) has been introduced in MOCAGE. It is a mass flux scheme, but the parametrization is slightly more complex than in our version of Tiedtke's method. Downdrafts are taken into account, as well as freezing and melting. All computations are one-dimensional, that is the surrounding columns have no influence (unlike in Tiedke's scheme where moisture convergence is crucial). To trigger (or not) convection in a column, a mixed air parcel is lifted from the ground to its lifting condensation level. If the difference between its virtual temperature $\overline{\theta}_v{}^{\text{mix}}$ and that of environment $\overline{\theta}_v$ is sufficiently high, then convection can be triggered off. The ability of the parcel to produce sufficient cloud depth is added to this condition. Shallow convection shall give at least a 500 m high cloud, and deep convection shall extend to 3 km.

Fractional entrainment (ϵ_u) and detrainment (δ_u) rates are computed according to Kain and Fritsch (1990). The formalism is based on the observation that the mixing between cloud and environment takes place close to the cloud. In the vicinity of clouds, mixtures of clear and cloudy air have an individual buoyancy which can be different from the mean buoyancy of the cloud. Every individual subparcel has its own virtual temperature. The scheme then postulates that all negative buoyancy mixture detrains from the cloud and that positive buoyancy entrains into the cloud. Then entrainment and detrainment rates depend on the thermodynamics of the updraft. The thermodynamic characteristics of the updraft are computed assuming that, except from precipitation processes, enthalpy and total water mixing ratio are conserved.

Finally, the intensity of the convection is controlled by a closure assumption. It is based on the removing of all convective available potential energy during an adjustment period, set to 3 h for shallow convection and between 0.5 and 1 h for deep convection.

2.3. Radon emissions

Radon (^{222}Rn) is a rare gas continually emitted by the radioactive decay of ^{226}Ra. It has no chemical activity and is not subject to wet or dry deposition; its own radioactive half-life is 3.8 days. Hence, radon is an interesting trace atmospheric constituent for studying transport in the troposphere since time scales are compatible, and for validating transport processes in MOCAGE, independently of chemistry, deposition and scavenging. The ^{222}Rn emissions may vary in time and space (see Dörr and Münnich, 1990), and the question of the accuracy of emissions is still topical. The range of the observed emission rates above non-frozen soils is between 0.7 and 1.5 atoms cm^{-2} s^{-1} (Liu et al., 1984), depending upon the geological composition of soils. Many authors have used ^{222}Rn as a tracer for GCMs or CTMs (e.g. Brost and Chatfield, 1989; Jacob and Prather, 1990; Feichter and Crutzen, 1990; Genthon and Armengaud, 1995; Stockwell and Chipperfield, 1999). A consensual value for radonic emissions seems to be 1 atom cm^{-2} s^{-1}, and we therefore chose this value for our simulations. The oceanic source is currently estimated to be at least 100 times smaller than above land surfaces, and has been neglected, following Li and Chang (1996), Stevenson et al. (1998) and Dentener et al. (1999). Finally, the observed emissions above frozen soils are drastically reduced by snow cover or soil freezing. In this work, a crude assumption was chosen: when surface soil temperature is negative, emissions are set to zero.

To avoid vertical gradients which are too strong within the PBL, emissions have been directly introduced into the five lower model levels (on average, over an altitude of 600 m). The subsequent increment in the mixing ratio ΔQ at level l is given by

$$\Delta Q(l) = 0.9 \times \Delta Q(l + 1)$$

where levels go from top to bottom.

These parameters (five levels, 0.9 coefficient) have been optimized for continental emissions in order to smooth the effects of 15-min injections and to reduce the influence of the depth of the first layer. Due to the σ coordinate, this depth varies in the model. Moreover, we may suppose that the five first levels of MOCAGE remain within the PBL most of the time. Measurements in Finland (Paatero et al., 1998) have shown that in winter the monthly averaged mixing height varied between 650 and 780 m on a continental site that is particularly stable due to its high latitude. In average, the depth of the five levels of MOCAGE is 600 m. This re-partition may hence produce little emission in the free troposphere.

2.4. Numerical simulations

Six-hourly ARPEGE operational analyses have been used to force the model during the 13 months from 1 December 1998 to 1 January 2000. Three experiments have been run:

- A simulation without subgrid transport process parametrizations (denoted NCV in the following).
- A simulation with the Tiedtke convection scheme (TDK).
- A simulation with the Kain–Fritsch–Bechtold convection scheme (KFB).

Both TDK and KFB include Louis' parametrization for turbulent mixing. After a 1-month run, 99.7% of the initial radon has disappeared, and the initial conditions have no further influence. The initial distribution of ^{222}Rn was hence set to zero, and spin-up time is considered to be 1 month. Simulations are then studied from 1 January 1999.

3. Climatological analysis

3.1. Global maps and zonal means

Jacob et al. (1997) present an intercomparison of a large number of model simulations of ^{222}Rn. Similar analyses were undertaken with MOCAGE results for zonal mean concentrations and mean concentrations at 300 hPa (Fig. 1) from June to August (JJA). This period is interesting when focusing on the effects of convection on ^{222}Rn distributions, since convective activity is more intense in the Northern Hemisphere where continents, and hence sources, are more extended. However, at variance with Jacob et al. (1997), it is noted that our meteorological fields correspond to the analysed meteorology of the actual year 1999.

3.1.1. JJA zonal means. For the two convection schemes the results are in good agreement with all the models tested in Jacob et al. (1997), both qualitatively and quantitatively. In this intercomparison, GCM with on-line mass-flux calculations or CTMs using archived convective mass flux are included: this is a first indication that the recomputation of mass fluxes within MOCAGE starting only from large-scale variables does not seem to have a strong impact on the intensity of vertical transport. In particular, deep convection in the tropics is well represented, with a greater activity for the KFB scheme. Its characteristics make transport of tracer from the low layers up to the high troposphere more efficient than in the TDK scheme, and give higher concentrations of ^{222}Rn in the upper equatorial troposphere. Mid-level convection at Northern Hemisphere mid-latitudes is also well represented. The difference between the two schemes is still due to the same reason: because transport from low layers is weaker in TDK, radon quantity is higher around 700–600 hPa.

The meridional gradient in the lower troposphere is less than that of the models tested in Jacob et al. (1997) or Stevenson et al. (1998) since their sources have been set to 0. or 0.005 atom cm^{-2} s^{-1} for latitudes beyond 60°. In our simulations, the average surface temperature remains positive up to roughly 75°N in June, July and August, so that sources are much more extended to the north.

3.1.2. Global maps at 300 hPa. Due to its short lifetime, the distribution of ^{222}Rn in the high troposphere is ruled by convective pumping that rapidly brings ^{222}Rn from the surface up to

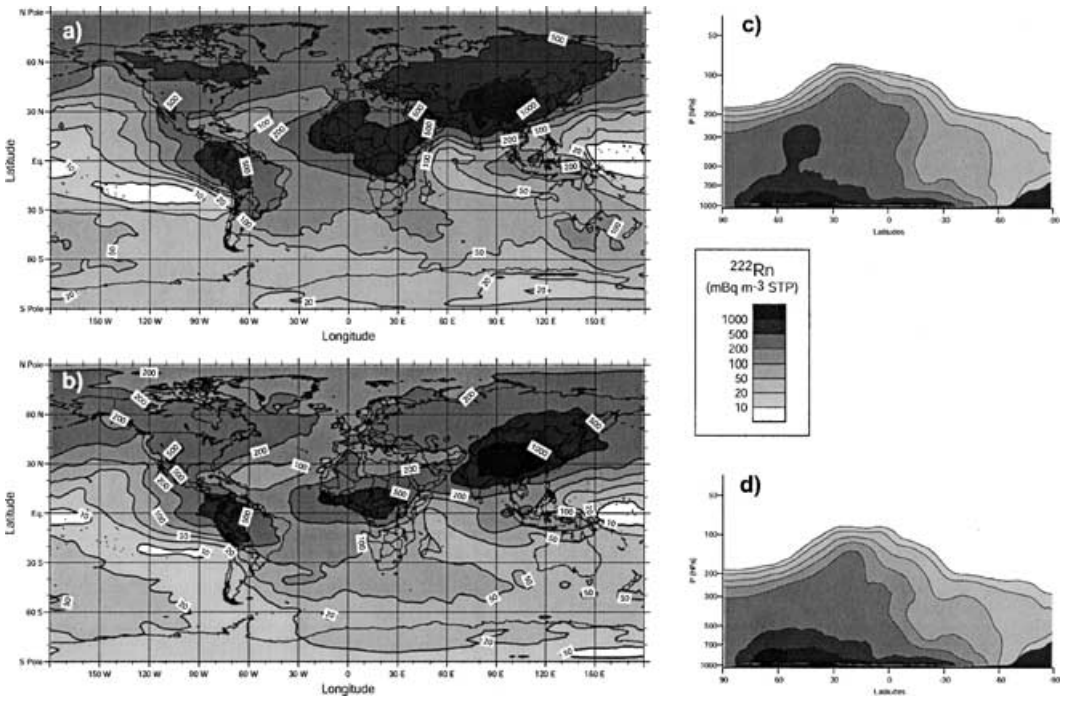

Fig 1. Mean radon concentration for June, July and August 1999 at 300 hPa: (a) TDK and (b) KFB (see text); (c) and (d) are the corresponding zonally averaged vertical profiles for TDK and KFB respectively.

altitude levels, and is relayed by horizontal large-scale transport. Again, MOCAGE simulations are consistent with those appearing in the intercomparison of Jacob et al. (1997) or Stevenson et al. (1998). The concentration of ^{222}Rn is particularly high above the African Inter-Tropical Convergence Zone (ITCZ). Above the Rocky Mountains, the Great Cordillera and the Himalayas the quantity is high too, probably in connection with large-scale ascent due to high orography; moreover, the 300 hPa altitude is closer to the surface in these regions.

3.2. Mean surface observations

The results obtained for the actual meteorological year 1999 have been used to compute monthly mean values at several surface observational sites. In this paper, we have selected four locations, characterized with markedly different ranges of variation of radon concentration: a continental one, a coastal one, an oceanic one and a site over Antarctica. Comparisons with observations are presented in Fig. 2. For every location, comparisons are made between observations and TDK, KFB and NCV simulations. Results correspond to a linear interpolation of model data at the precise location of the station:

Socorro (34° N, 106.5° W). Socorro is a continental site, in New Mexico, USA. Figure 2a compares the model monthly averages for 00:00 UTC with the climatology of Wilkening (1959), based on 6-yr observations (1951–1956). A good agreement is found, despite a slight underestimation in the winter months. For NCV, a general overestimation of about a factor of 2 is found. This overestimation is almost constant during the year, suggesting that the bias is due to the lack of vertical mixing. However, it should be noted that measurements were made at 1 m above ground, whereas MOCAGE values correspond to an average concentration in the 40 m thick surface layer.

Livermore (37.5° N, 121.5° W). Livermore is located on the Pacific Coast in California, USA. The simulation of coastal sites is a challenge for a global model: the contrast between the ocean (no emissions) and the continent results in strong gradients along the coastline, as seen at the model horizontal resolution. However, as illustrated in Fig. 2b, MOCAGE gives a satisfactory representation of the annual cycle, especially concerning the increase in autumn. A tendency to overestimate the observational climatology is noted, however: the averaged bias is 1.3 Bq m^{-3} standard temperature and pressure (STP) for KFB and 1.1 Bq m^{-3} STP for TDK, for NCV the bias peaks up to 2.2 Bq m^{-3} STP. As already remarked in Jacob and Prather (1990), this climatology is based on only 1 yr of observations; interannual variability could explain part of the discrepancy between the 1999 cycle and the observed one.

Crozet Island (46° S, 51° E). Crozet is a French island, situated in the sub-Antarctic Indian Ocean, 2800 km from the African coast. In Fig. 2c the representation of the annual cycle is in close agreement with the observations of Polian et al. (1986). In particular, the high concentration in the Austral winter (July–August) is a result of strong radonic events, similar to the ones illustrated in the next section. Taking into account convection and turbulence appears to be essential during this period. The amplitude of the annual cycle is greater in the model than in the observations, probably again partly because observed monthly means are a climatology over 25 yr.

Dumont d'Urville (66° S, 140° E). Dumont d'Urville is a French station located on the coast of Antarctica. Radon measurements are also from Polian et al. (1986). At variance with other sites, the simulation is not in agreement with observations (Fig. 2d). Though levels are in the correct range, the simulated annual cycle presents variations which are out of phase with observations; in the Austral summer, for instance, MOCAGE largely underestimates radon concentrations. Among other references, Genthon and Armengaud (1995) have already mentioned such discrepancies and, to our knowledge, no model has ever presented a fully satisfactory simulation of radon in Antarctica.

First of all it is interesting to remark that radon measured at Dumont d'Urville, and more generally above Antarctica, comes from remote continental regions. The surface temperature indeed always remains negative and, as already mentioned in Section 2, ice and snow cover prevents radon from being emitted locally. The summer maximum appears to be a robust and recurring feature, minimizing the possibility of it being an artefact induced by local pollution, for instance. At Dumont d'Urville, we may hence suppose that radon comes from Australia, New Zealand or Africa. Polian et al. (1986) hypothesized that the relatively high concentrations observed at Dumont d'Urville were due to "radonic storms" bringing in suddenly radon-rich air masses by a process of advection near and over the sea surface. In summer, they explain that radon-rich air masses travel higher in the atmosphere: vertical transport by deep convection above continents, advection in altitude and finally subsidence above Antarctica. The main point is that measurements in Tasmania were found to be lower than at Dumont d'Urville, leading them to "rule out the possibility of southward transport of radon at sea level" in the summer. According to Polian et al. (1986) a possible cause for the discrepancies between model and observations could be that vertical downwards transport is poorly accounted for in models.

The present simulations, with both convection schemes, indicate, however, that the total column amount of radon is not sufficient to account for the levels observed at the surface. Thus it appears that the problem is not sensitive to the representation of vertical transport.

The lack of radon in the models at the surface at Dumont d'Urville could hence be due to a bad representation in the meteorological analyses, or in general circulation models, of synoptic activity at high latitudes. In particular, it is worthwhile considering the surface pressure at Dumont d'Urville, both for observations and in the analyses throughout the year 1999; Fig. 3 presents the monthly averaged difference between the two. There

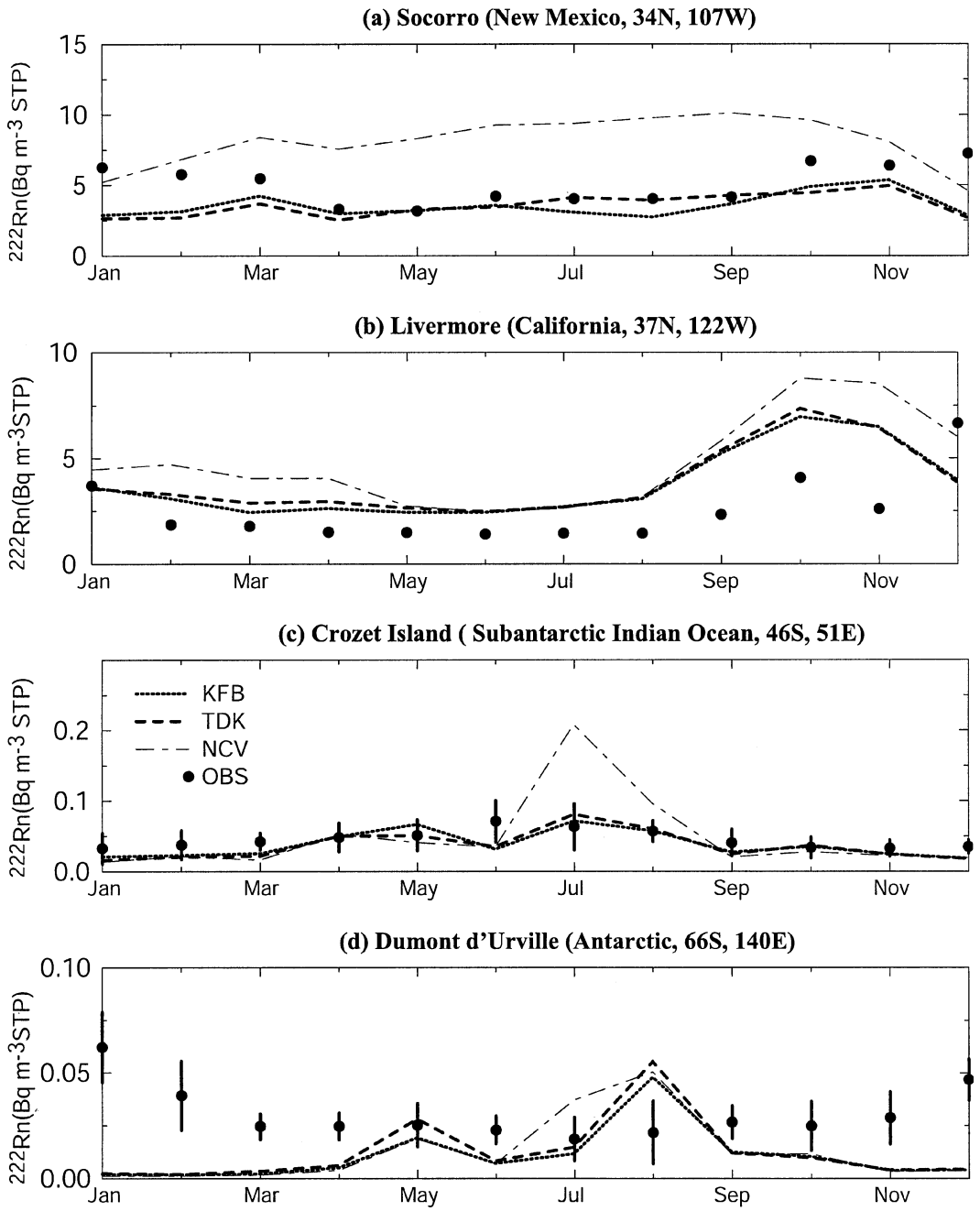

Fig 2. Seasonal evolution of surface ^{222}Rn (monthly means for 1999) for TDK (bold dashed line), KFB (bold dotted line), NCV (thin dashed line), and observations (black circles) in several locations worldwide: (a) Socorro, USA; (b) Livermore, USA; (c) Crozet Island, sub-Antarctic Indian Ocean; (d) Dumont d'Urville, Antarctica. Vertical bars denote $\pm 1\sigma$, where σ is the standard deviation of the monthly mean of observations, when available. For clarity, different scales for ^{222}Rn concentrations are applied.

is a clear annual cycle in the bias: during local summer, the model overestimates surface pressure, while it the opposite pertains during the local winter.

A more precise look at specific cases emphasizes the fact that summer lows are weaker in the model than in the observations. Either their intensity or their position is not well represented. In the first case, the radon is unlikely to reach the correct location. In the second case, the advection velocity is not correct, and the radon concentration will also be incorrect. For instance, if the depression is not low enough, the flux will be too slow and radon will be submitted to too much radioactive decay in the model, and simulated radon concentration will be too low.

Our hypothesis is that radon-rich air is brought in by lows coming closer to the coast during the summer, because of the

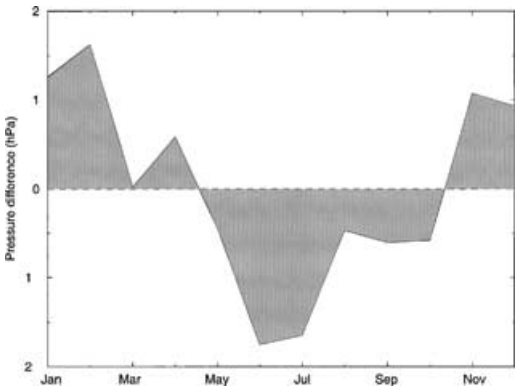

Fig 3. Monthly mean bias between ARPEGE meteorological analysis and observations for surface pressure at Dumont d'Urville in 1999 (66° S, 140° E).

smallest extent of sea ice. Circum-Antarctic polar lows are indeed maintained by surface latent and sensible heat fluxes. When a particular polar low moves southward and meets sea ice, it tends to weaken. One reason for this is that sea ice significantly reduces ocean–atmosphere heat exchanges due to its insulating effect. Thus polar storms originating in Antarctic seas generally cannot penetrate the continent when sea ice spreads far off the coast (Salas-Mélia, personal communication). Dumont d'Urville is located on the coast of the Antarctic continent. Thus, in summer, when the sea ice is less extended, lows may come closer to the station than in winter. They are hence able to bring more radon to this station, since radioactive decay is less efficient because of faster transport. This seems to be a good explanation for the higher values in summer at Dumont d'Urville than in winter, contrary to Crozet and Amsterdam for instance.

Moreover, for 1999, the extent of the sea ice in the forcing model ARPEGE is represented using climatological data, and the (satellite) observed interannual variability has been proved to be extremely high (Gloersen et al., 1992). The crude representation of the extent of sea ice in the forcing model is likely to be responsible for the biased modelling of the flux and thus of the radon concentration.

To illustrate a possible scenario, we have chosen here the example of the situation of 3 and 4 December 1999 (Fig. 4).

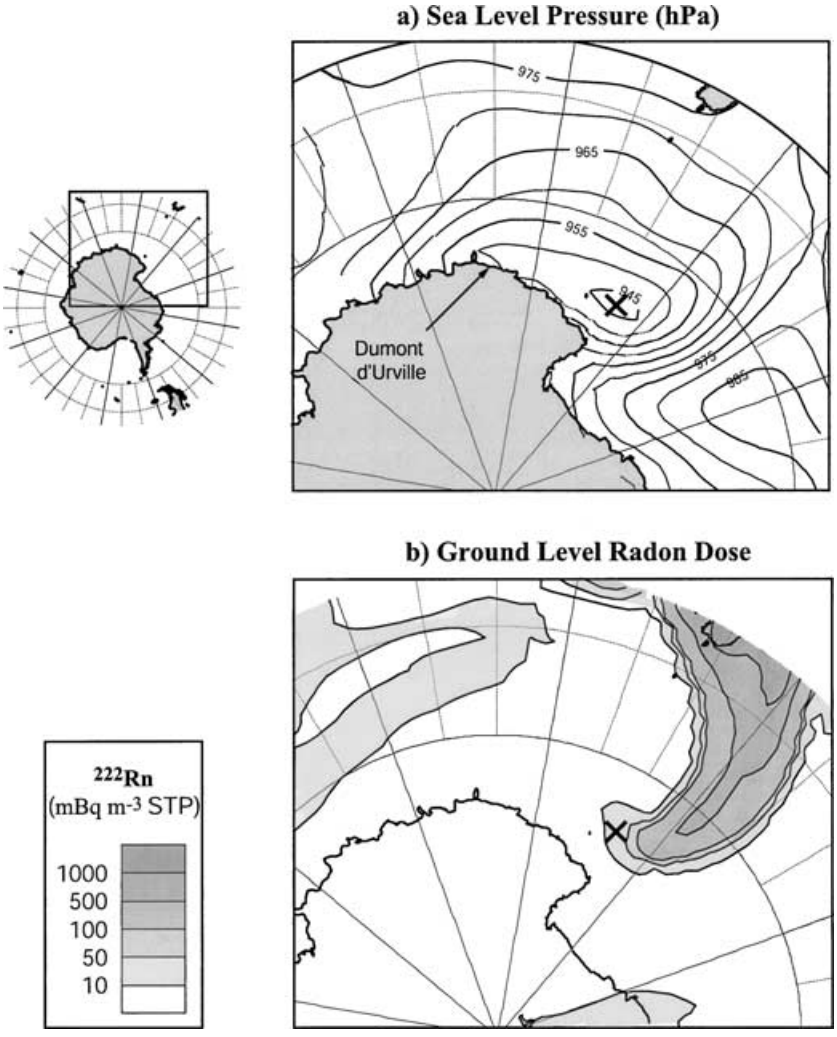

Fig 4. Surface pressure in the ARPEGE meteorological analysis (a) and ^{222}Rn concentration simulated by MOCAGE in KFB (b) at the surface, for 4 December 41999 12:00 UTC. The cross indicates the location of the low (945 hPa) influencing the tongue of radon coming from Australia. This pressure level was in fact observed at Dumont d'Urville, indicating that the low (and associated ^{222}Rn transport) was actually closer to the coast.

A relatively important low is arriving at Dumont d'Urville on 3 December at 12:00 UTC. This low is represented by the model and is reported in the observations. But the evolution of this low is not well reproduced: on 4 December the observed pressure at Dumont d'Urville was 945 hPa whereas the simulated pressure is 951.2 hPa. Concerning radon, a tongue of tracer comes from Australia and New Zealand very close to Dumont d'Urville on the 3 December but is taken away by the cyclonic flux on the 4 December. The location or the intensity of the low (or both) is bad on that day, and we may suppose that some radon has been arriving in reality at Dumont d'Urville but has not been represented in the model. Such an event would have been enough to have given a much higher monthly mean concentration at Dumont d'Urville.

3.3. Altitude observations

3.3.1. Hawaii. Kritz et al. (1990) reported measurements of radon concentration at altitude in July and August. Seventeen of these measurements were made in the vicinity of Hawaii, around 200 hPa. The major features of these observations is a high spatial and temporal variability, with unexpected high values up to 1.5 Bq m^{-3} STP. Kritz et al. (1990) showed that these high values were due to deep convection above Eastern Asia, followed by rapid advective transport in the high troposphere, especially in the subtropical westerly jet. We have computed the simulated quantity of ^{222}Rn at 200 hPa in the vicinity of Hawaii for June, July and August 1999. A detailed evaluation is impossible using this dataset only, but we aim here to testing the ability of the model to reproduce the main features of these observations.

First, the mean map at 200 hPa for these three months (Fig. 5a) shows a high gradient to the northwest of Hawaii: the model reproduces the rapid advective transport of convected air above Eastern Asia. The spatial variability is thus well represented. In particular, a sharp gradient in the vicinity of Hawaii takes place on 10 June 1999 (see Fig. 5b). Figure 5 represents the model results only for the KFB scheme, but results for the TDK scheme are very similar.

The time variability is satisfactory too; the daily radon dose at 200 hPa above Hawaii presents variations of more than one order of magnitude (Fig. 6). This time variability is also obvious when comparing the difference between values for whole

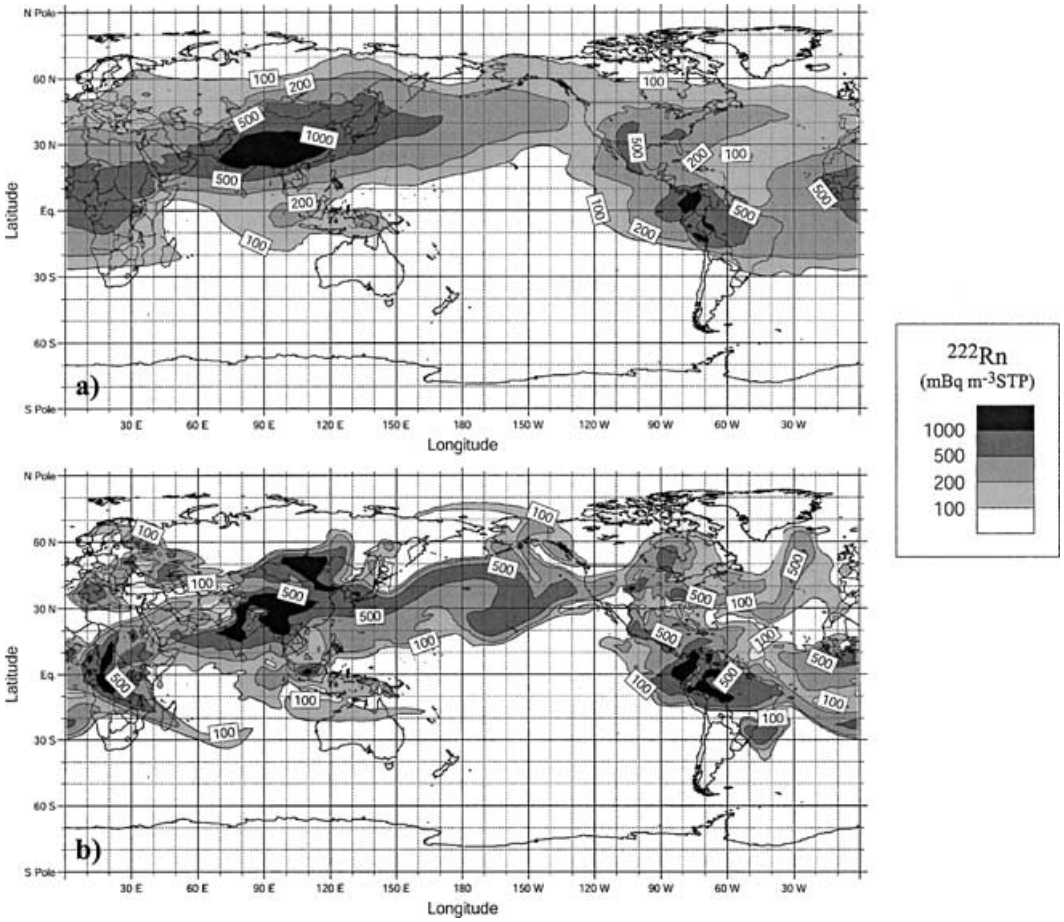

Fig 5. ^{222}Rn concentration simulated at 200 hPa in KFB: (a) June–July–August 1999 mean; (b) for 10 June 1999 00:00 UTC.

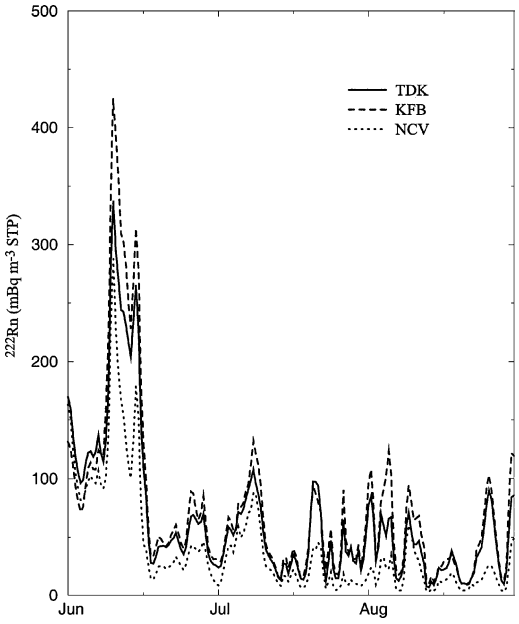

Fig 6. June–July–August 1999 ^{222}Rn concentration at 200 hPa for TDK (solid), KFB (dashed) and NCV (dotted), averaged over a domain centred on (155°W, 21°E) in the vicinity of Hawaii.

summer (JJA) and for only the month of June. In June, the NCV simulation gives high values, similar to those calculated with KFB and TDK, suggesting that synoptic-scale transport has a greater impact during this period. The time variability therefore concerns the type of transport itself.

Moreover, for JJA, the median of modelled values in the vicinity of Hawaii (170° to 150°W, 18° to 25°N) is 65 mBq m^{-3} STP, which is much lower than the observed median, 140 mBq m^{-3} STP. In June, the median reaches 110 mBq m^{-3} STP, which is still lower, but more in agreement with the observations.

Despite a fair representation of spatial and time variability, concentrations are much lower than those observed by Kritz et al. (1990). The statistical significance of the estimation of the median on a set of only 17 measurements is probably questionable, given this strong variability. However, over the whole region where the radon concentration was measured no simulated quantity at any model point exceeds 770 mBq m^{-3} STP, suggesting an underestimation of the model. We studied several hypotheses to explain this discrepancy.

The first one is based on the uncertainties in the representation of Hawaiian emissions. There are several small islands which are subgrid at the model resolution and are treated as ocean grid points with no emissions. A simple experiment was set up, in order to fiddle with radon emissions in the model grid point encompassing Hawaii and neighbouring islands. First, we have introduced the emissions that correspond to the approximate total land surface; second, as a sensitivity study, we have tripled this amount. With no surprise, at the altitude of the measurements the influence of these local emissions is almost nil, whether it was for the "realistic" rate of emission or for the tripled one. This is certainly due to the fact that high-altitude winds here are strong westerly jets, bringing locally emitted radon rapidly out of the observational domain. The representation of Hawaiian radon emissions is not connected to the underestimation of the radon doses in altitude.

The second hypothesis lies on the demonstration by Kritz et al. (1990) that deep convection followed by subtropical jet winds was responsible for unexpected high-altitude radon concentrations. It may indeed be possible that deep convection is not strong enough to transport ^{222}Rn from the ground up into the high troposphere as efficiently as in reality. We conducted another experiment, arbitrarily increasing convection intensity by multiplying convective mass fluxes by a factor of 4 in TDK. Results still do not show maximum concentrations as high as the observed 1.5 Bq m^{-3} STP.

Jacob et al. (1997) have already mentioned that all the models tested in their intercomparison largely underestimated radon concentrations over Hawaii. Given the probable origin of high quantities of radon above this region, their hypothesis was an unknown source of ^{222}Rn over Eastern Asia—this also being consistent with observations of very high ^{210}Pb (the product of the radioactive decay of radon) deposition fluxes in Asia, compared with other continental sites in Europe and in the United States. In the light of our new experiments, we believe that this explanation remains valid.

3.3.2. Comparison with a climatological vertical profile. A large number of available measurements of vertical radon profiles were gathered in Liu et al. (1984). This compilation provides estimates for the mean vertical profiles for continental sites in winter, spring or autumn, as well as in summer. Since most of the profiles in the climatology were summer ones, we chose to focus our comparison on the summer profile; the two other ones rely on too few profiles to be quantitatively trusted. In addition, most of the observed profiles were obtained over the continental United States. Thus, we compare the summer climatological profile with a mean vertical profile computed with MOCAGE for the months of June, July and August 1999 and over a box covering a large region of the continental United States (109° to 89°W, 31° to 51°N) at 15:00 local time, corresponding to the majority time and location of profiles.

As illustrated in Fig. 7, the simulated radon profiles with TDK and KFB are close to the climatological one, and almost within the variability bars over the whole tropospheric column. The main difference between the two convection schemes is that the effect of convection is stronger in the lower layers in KFB than in TDK. For instance, at 2 km of altitude, the mean concentration in TDK is 1.3 Bq m^{-3} STP and only 750 mBq m^{-3} STP for KFB. By contrast, at 10 km, KFB gives 550 mBq m^{-3} STP, whereas TDK yields 300 mBq m^{-3} STP. Another interesting feature is that the simulated profile without convection or turbulence (NCV) is drastically different from the observed one; despite small

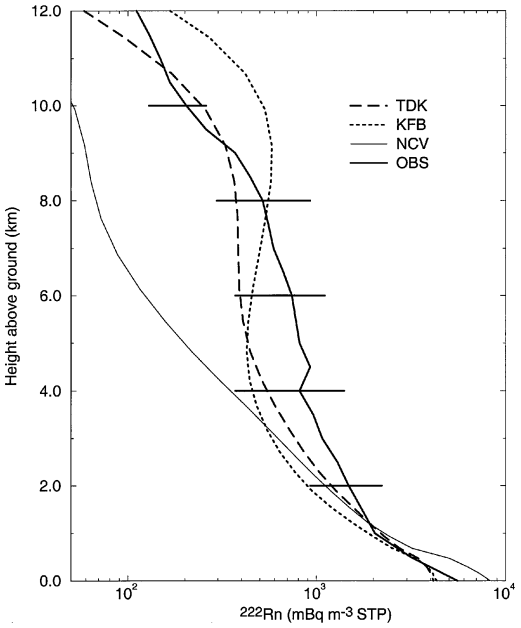

Fig 7. ^{222}Rn mean summer vertical profile over the continental United States: climatology of Liu et al. (1984) and associated variability, solid line; TDK, dashed line; KFB, dotted line; NCV, thin solid line.

differences between KFB and TDK, subgrid vertical transport is essential.

4. Case studies

4.1. Amsterdam Island

Until now, model outputs have been compared with observations that do not correspond to the actual year of our simulations (climatology or another year). Radon measurements for the year 1999 at Amsterdam Island have been obtained from M. Ramonet (personal communication). These measurements are performed at 2 m above the ground every 20 min; raw data are averaged to provide 2-hourly values in order to screen out undesirable high-frequency noise in the signal. These data are very useful to further validate transport in our model, allowing us to assess the ability of MOCAGE to account for specific events. The horizontal resolution of the model at this location is 2°. The simulated radon doses for Amsterdam Island correspond to a linear interpolation from the MOCAGE grid at the longitude and latitude of the island (77.3°E, 37.5°S).

4.1.1. Results for 1999. Figure 8 presents the evolution in time of the ^{222}Rn concentration at Amsterdam Island, as computed in the model for the two convection schemes on the one hand, and as observed on the other hand. Model outputs are archived every 12 h; instantaneous simulated values are compared with instantaneous measurements.

Both convection schemes lead to mean concentrations which are too low. Throughout the whole year 1999, the observed mean radon concentration is indeed 38.5 mBq m^{-3} STP. TDK gives 25.5 mBq m^{-3} STP (34% less than in the observations) and KFB 20.3 mBq m^{-3} STP (47% less than in observations). The discrepancy between the model and the observations is, however, not systematic. The distribution of the observations shows that 95% of the concentrations are below 92 mBq m^{-3} STP. We have divided the values between "low" (below this threshold) and "high" (above this threshold) concentrations. The average of the high values is 157 mBq m^{-3} STP for the observations, 172 for TDK and 148 for KFB. The global underestimation is essentially due to the low values, which are too low in the model. An explanation can be found in the fact that high values are related to more rapid transport from source regions than in the case of low values. To cover the same distance, the more rapid transport is, and the less impact errors in the model (smoothing by numerical diffusion, only partially alleviated by the radioactive decay, etc.) have on the simulated radon levels.

The evolution in time of the radon simulations is similar for the two experiments, even if, as previously seen in the climatological vertical profiles, KFB gives concentrations generally smaller than TDK in the low atmosphere. Radon observed at Amsterdam Island comes mainly from the east of the African continent; it is emitted at the surface then submitted to convection and transported by low- to mid-tropospheric winds above Amsterdam Island. As the KFB scheme takes more radon from the ground up to the high troposphere, the tracer quantity transported to Amsterdam Island is hence lower than in TDK.

Another important aspect in the comparison is the correlation between the simulated doses and the observations. This is especially important here, because the observed radon concentrations vary drastically through the year; the surface ^{222}Rn level is generally low, but on occasions concentrations peak up to approximately 370 mBq m^{-3} STP. The correlations we obtain are quite satisfactory: in KFB, the year-round correlation is 0.52 and 0.49 in TDK (slightly lower than that of Dentener et al. (1999), but computed on instantaneous values), and only 0.13 for NCV. The model has some ability to reproduce the temporal variability of the radon concentrations, and is able to detect exceptional events.

4.1.2. Local winter period. We now analyse the model results in the local winter months of June, July and August (JJA) 1999. Radon observed above Amsterdam Island comes mainly from the African coast, from which it is carried away by westerly winds and mid-latitudes eddies. The more rapid the eddy is, the greater the radon concentration, as there is less radon destroyed by radioactive decay. Most of the time, radon transport takes place in the middle troposphere, the surface concentration remaining low over the ocean; the maximum concentration is found around 400 hPa (see Fig. 9). Under certain circumstances the surface concentration becomes very high; such episodes are called "radonic storms" (Polian et al., 1986). These winter radonic storms are reported in the observations and are well reproduced by the model. Correlation with the observations

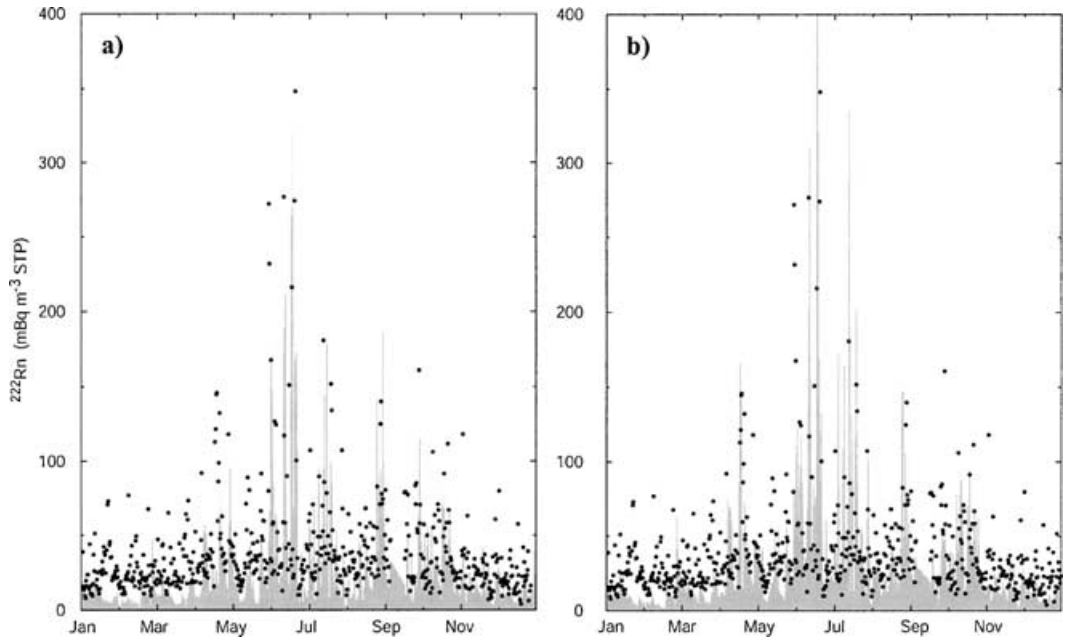

Fig 8. Simulated and observed (black dots) surface 12-hourly ^{222}Rn concentrations at Amsterdam Island (37°S, 77°E) for 1999: (a) KFB; (b) TDK.

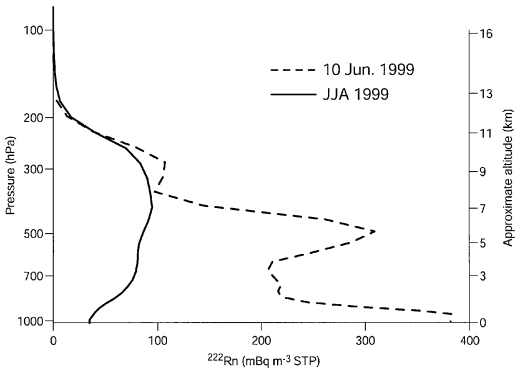

Fig 9. ^{222}Rn profile simulated above Amsterdam Island in KFB: June–July–August 1999 mean, solid line; 15 June 1999 00:00 UTC, dashed line.

is indeed better in JJA than throughout the whole year (0.58 for KFB), and, as already mentioned, the high values of the ^{222}Rn mixing ratio are nicely captured.

We describe here a specific radonic storm at Amsterdam Island. The chosen episode occurred on 15 June and is illustrated in Figs 10 and 11; the model simulation is very realistic compared with the local observations. As for Crozet and Kerguelen islands (Balkanski and Jacob, 1990), the Mascareigne High plays a major role in the Amsterdam Island radonic storms. Firstly, on 12 and 13 June, this anticyclone comes closer to the African coast than usual and surface concentrations near the coast on these days are especially high. In combination with a large mid-latitude depression, a very rapid flow develops at the surface. A plume, quite extended on the horizontal but extremely sharp on the vertical, is exported from the continent, starting on 12 June. Due to rapid advection almost within the marine boundary layer, it arrives in Amsterdam Island on the 15 June. On that day, the radon profile above Amsterdam Island (Fig. 9) is notably different from the mean; it emphasizes the primary role of low-layer advection in this storm. Latitudinal and longitudinal sections around Amsterdam Island (Fig. 10) illustrate the geometry of this tongue of advected continental air. This example seems quite representative of the conditions required to develop the most marked radonic storms.

4.2. Mace Head

Mace Head is located on the west coast of Ireland at (53.2°N, 9.54°W). As already mentioned for Livermore, the simulation of coastal sites is difficult due to the sharp contrast between oceanic and continental emissions. In MOCAGE, every grid cell is either land or water (ocean, sea, lakes). Both for the 2° resolution and the 1° resolution MOCAGE domains, the grid cell of Mace Head (defined as the cell in which the exact longitude and latitude fall) is land. In order to represent the concentration at the coastline, we chose to study the point in between the Mace Head land grid cell and the neighbouring ocean grid cell at the same latitude. The location of Mace Head in Europe allows us to study the impact of the model resolution since the site is within the 1° resolution domain of MOCAGE, which spans from (20°W, 30°N) to (40°E, 60°N).

4.2.1. General results. We focus in this section on the model performances with both schemes, KFB and TKD, at the horizontal resolution of 1°. The key characteristic of the evolution in time of radon at Mace Head is the influence of the synoptic

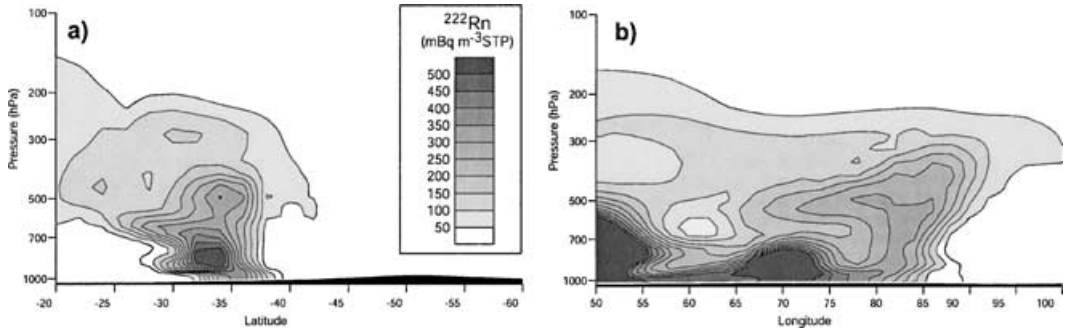

Fig 10. Simulated vertical cross-sections of ^{222}Rn concentrations in the vicinity of Amsterdam Island for 15 June 1999 00:00 UTC (KFB): along the 77°E meridian (a) and along the 37°S parallel (b).

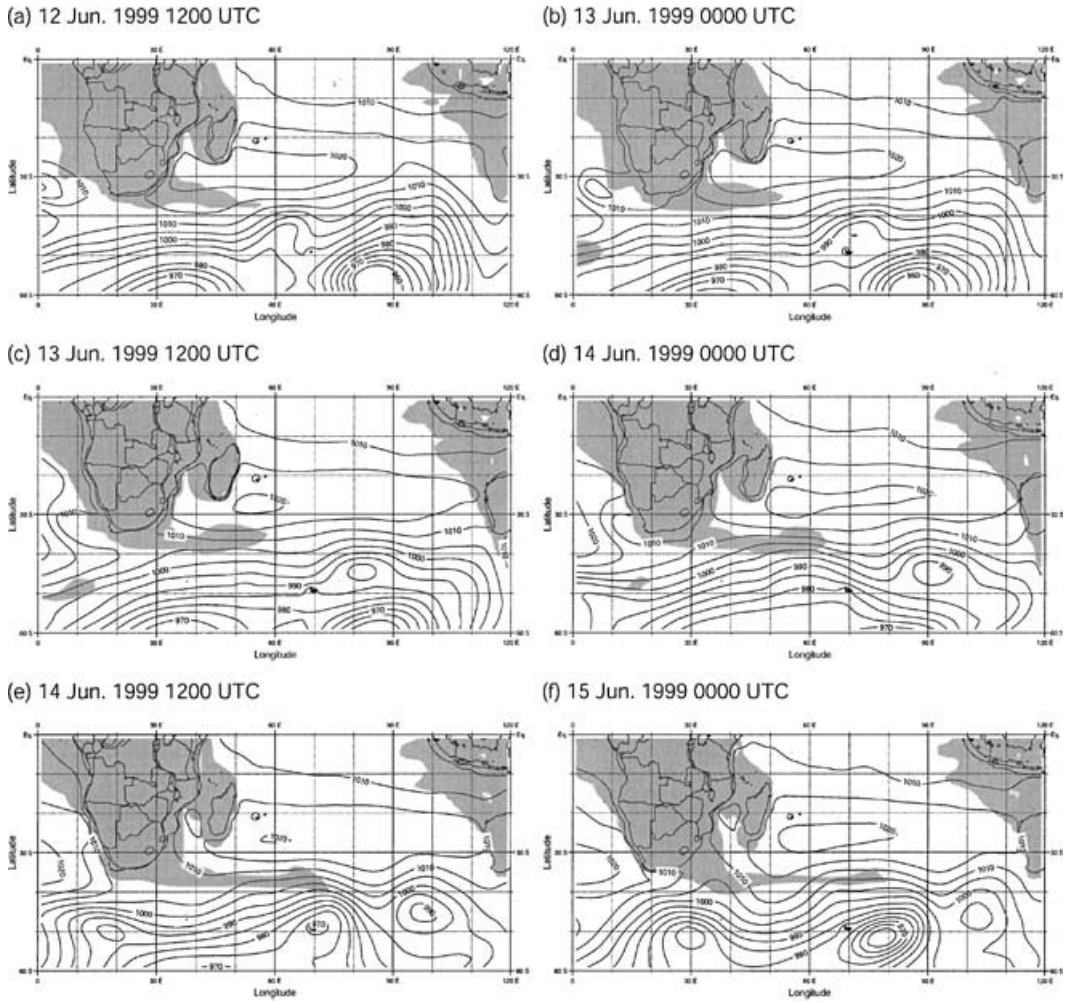

Fig 11. Surface pressure (isolines, hPa) and simulated ^{222}Rn concentration in KFB (shaded areas correspond to doses higher than 300 mBq m^{-3} STP), from 12 June 12:00 UTC (a) to 15 June 00:00 UTC (f).

scale. The concentrations are only weakly affected by the representation of convection: NCV, KFB and TDK present similar behaviours. Indeed, doses in NCV are higher due to the lack of vertical mixing. This tends to suggest that subgrid transport is less important here than in other locations, as it does not determine primarily the main variations. Moreover, the correlation between zonal wind and simulated radon concentration is significant (−0.6). This is expected (Biraud et al., 2000): when wind comes from the west (positive zonal wind), radon-poor oceanic air is brought; and vice versa, under easterly winds (negative

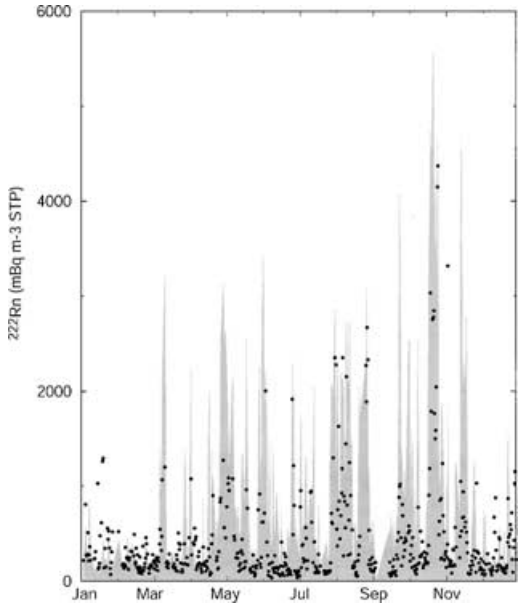

Fig 12. Simulated and observed (black dots) surface 12-hourly ^{222}Rn concentrations at Mace Head, Ireland (53.2°N, 9.5°W) for 1999 and in KFB.

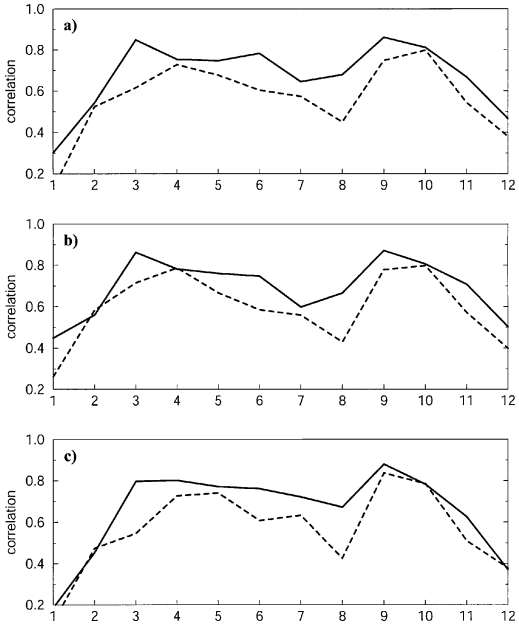

Fig 13. Monthly mean correlation coefficient (r) between observations at Mace Head (53.2°N, 9.5°W) and model for KFB (a), TDK (b) and NCV (c). Solid lines are for the 1° horizontal resolution domain, while dashed lines correspond to the 2° resolution.

zonal component), radon-rich continental air arrives at Mace Head. Such a high correlation again illustrates the fact that the synoptic flow is the key driving factor in the temporal evolution of radon here.

As illustrated in Fig. 12, simulated and observed mean values at Mace Head are relatively low. This is of course due to the fact that flow is generally westerly and air masses come from the ocean. Thus, the annual mean of observations is 400 mBq m^{-3} STP. For MOCAGE, the corresponding values are too high: 710 (respectively 760) mBq m^{-3} STP for TDK (respectively KFB). Without convection, the discrepancy is even higher (960 mBq m^{-3} STP). As already mentioned, the proximity of the coast may be an important factor. If the simulated levels are biased, the variations are quite correctly captured: the linear correlation coefficient between the model and the observations throughout the year is 0.71 in the three simulations KFB, TDK and NCV. Looking more precisely into the monthly evolution of the correlation, presented in Fig. 13, it appears that correlations are high, except for the winter months: December, February and especially January. This marked degradation in model performance is due to a high-concentration event not reproduced by the model (see next section). The correlations are particularly high in spring and autumn, for every scenario. During these seasons, strong westerlies, and hence synoptic-scale transport, dominate. For every month and every experiment the simulation at 2° gives similar results (not shown) with lower, but significant, correlations than at 1°.

4.2.2. High-concentrations episodes. As mentioned above, concentrations at Mace Head are relatively low (around 400 mBq m^{-3} STP) for a site in Europe, due to its location. However, on occasions the concentrations are much higher, up to 4.8 Bq m^{-3} STP in 1999. As for Amsterdam Island, we defined "high" values, as those higher than 95% of the total observed values; with this definition, a peak corresponds to a concentration greater than 1.11 Bq m^{-3} STP. Except for two events in 1999, all the other high-concentration events are captured by the model. We investigate here the type of meteorological conditions that are connected with such events.

First of all, high values may occur throughout the year, except maybe in winter; this is in sharp contrasts with the "radonic" storm-type events we have described for other sites. The duration of these events is quite variable, ranging from 1 to 10 days. We have studied every episode that occurred in 1999, relating it to the specific meteorological context using ARPEGE operational analyses (that, in turn, correspond to the forcings of MOCAGE and hence are fully consistent with our simulations). In the end it is possible to define different characteristic meteorological conditions leading to high radon concentrations at Mace Head. The usual situation has already been mentioned. When lows are arriving from the Atlantic, inducing a westerly flow, the concentrations remain low, especially throughout the winter. An example of such a situation occurred on 24 February (Fig. 14), with a low centred over Iceland.

A first situation is when a high is located over the British Isles, as on 24 and 25 June. This episode is reported in Fig. 15. The high induces a limitation of the extension of vertical transfers

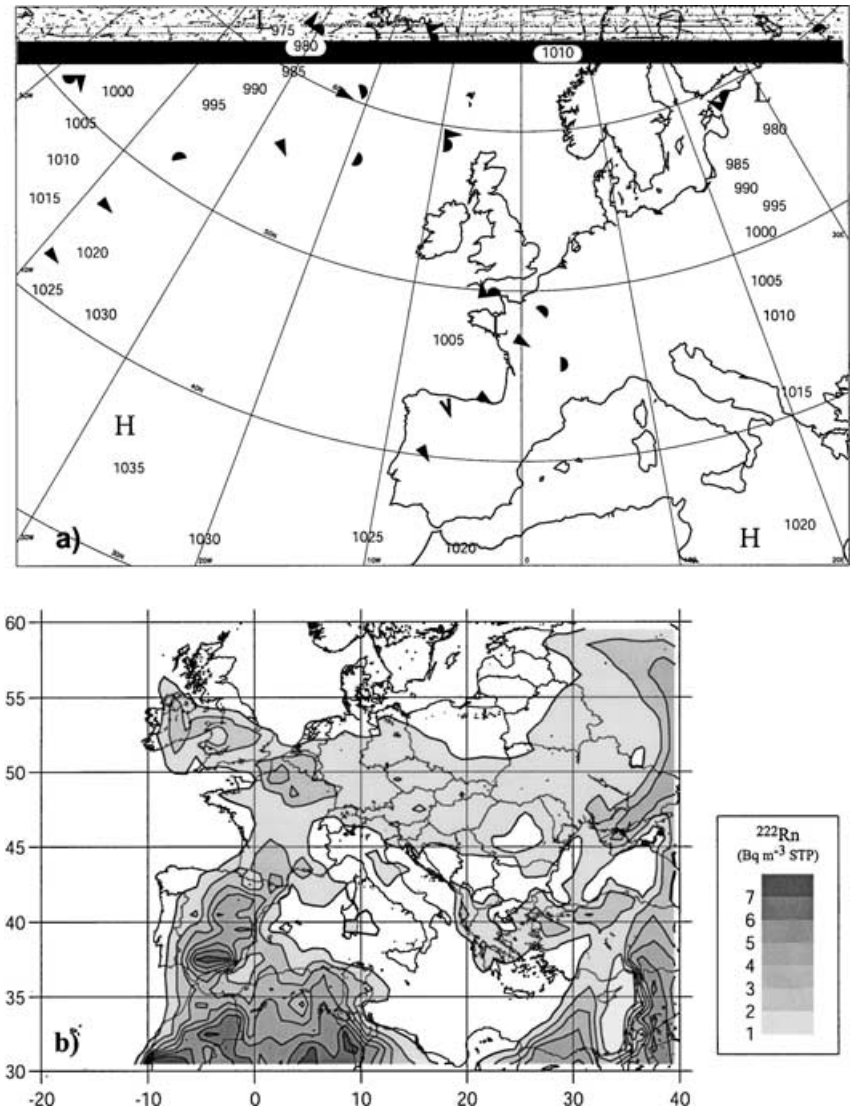

Fig 14. Mean sea level pressure analysis (ARPEGE) and ^{222}Rn ground concentration simulated by MOCAGE (KFB) for 24 February 1999 12:00 UTC.

and prevents oceanic air from coming over Mace Head. Thus, local emissions make a major contribution; they rapidly drive the ground radon concentration to very high values (+1.48 Bq m^{-3} STP in 12 h). As soon as the low located to the northwest of Ireland comes closer (on 26 June at 12:00 UTC) the direction of the flow becomes northwesterly, and concentrations drop. MOCAGE captures this episode well, particularly as far as the chronology is concerned. For instance the marked decrease on 25 June at 00:00 UTC is seen by the model at 1° horizontal resolution, even if it is less sharp than in reality. At 2° of resolution, MOCAGE is not able to account for this sudden decrease; more generally, at this resolution results are still quite satisfactory but the evolution of concentrations is as expected smoother than for 1°. The same type of situation also prevailed for the high radon episodes of 27 to 29 April, 27 to 29 July and 14 to 15 October 1999.

Another possible situation is the combination of a low located in the near Atlantic, west of Ireland and a high, located over western continental Europe. The flow coming over Ireland is southeasterly. A typical situation of this kind occurred from the 17 to 22 October 1999 (Fig. 16). The high, which was previously located above the British Isles on 14 and 15 October, moves to the northeast. As long as the low remains west or south of Ireland (the high preventing the low pressures from going further), emissions coming from continental Europe and the Britain arrive at Mace Head. In other words, radon concentrations have remained high since the 14 October but the source of radon has changed: from local, it becomes distant. During this episode, concentrations vary (depending upon the precise location of the low- and high-pressure systems), but the direction of the flow stays between southeast and east, bringing radon-rich air masses. Concentrations over 1.85 Bq m^{-3} STP have been observed, which

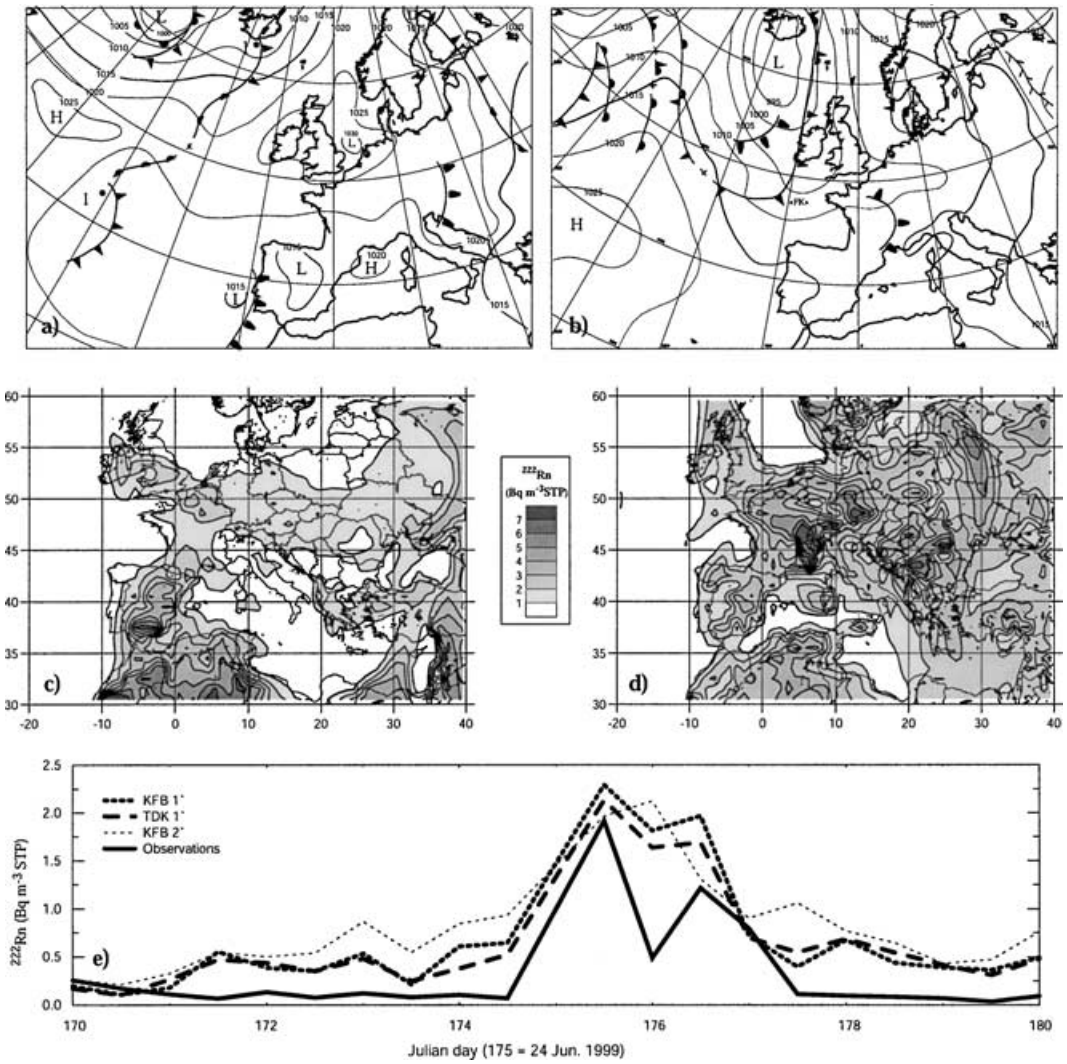

Fig 15. Mean sea level pressure analyses (a and b) and ^{222}Rn ground concentrations simulated by MOCAGE (KFB) (c and d) for 24 June 12:00 UTC and 26 June 12:00 UTC respectively. Panel (e): ^{222}Rn ground concentration at Mace Head during the peak period (see text) in observations for KFB at 1° resolution (dotted line), TDK 1° (dashed line), KFB 2° (thin dotted line) and observations (solid line).

is nicely reproduced by MOCAGE at 1° resolution and, again, to a lesser extent at 2° resolution. Such a type of situation also occurred in early June 1999, in early August and on 24 and 25 August.

We have just described two of the most characteristic meteorological situations that lead to high radon concentrations at Mace Head. But the prevalence of this type of situation doesn't systematically imply high radon. For instance on 10 to 11 November a high is located above the British Isles with a maximum pressure of 1045 hPa. The ground temperature was around 10°C, hence the ground emits and the wind is low and comes from the east. Despite this very auspicious context, the observed radon ground concentration increases, but hardly reaches 740 mBq m^{-3} STP. MOCAGE gives a very high radon dose during this period, as for the other events of this kind. It is possible that local processes may occasionally play some role and interfere. Similar conclusions were reached for instance by Chevillard et al. (2002). MOCAGE resolution is too coarse to account for sea breezes, for instance, that can bring clean oceanic air to the site. Vice versa, some observed peaks are not seen by the model, whatever the resolution. During the episode of 20 January, the radon dose reaches 1.3 Bq m^{-3} STP; the flow is steady and southwesterly, and MOCAGE simulates low radon. Again, local processes are a probable cause of the discrepancy.

To conclude, MOCAGE is able to reproduce quite accurately the variations of ^{222}Rn concentration at Mace Head, all the more if the horizontal resolution is high. Through 1999 we have distinguished two types of meteorological situations that lead to high radon episodes; the synoptic context is most of the time the principal driving force behind the evolution in time of the

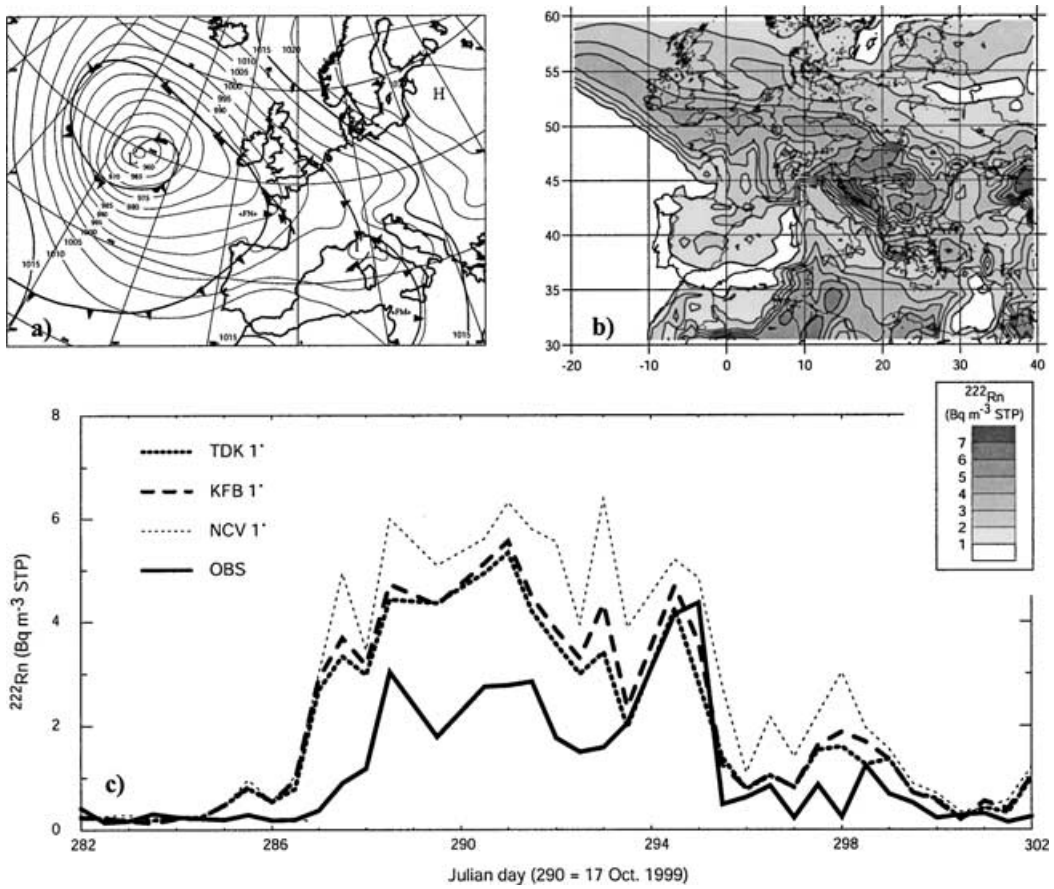

Fig 16. Mean sea level pressure analyses (a) and ^{222}Rn ground concentrations simulated by MOCAGE (KFB) (b) for 21 October 12:00 UTC. Panel (c): ^{222}Rn ground concentration at Mace Head during the peak period (see text) in observations (solid line) and in KFB (dotted line), TDK (dashed line), and NCV (thin dotted line) at 1° resolution.

concentration. However, for this site, local circulations such as breezes, that the model cannot reproduce, sometimes interfere and alter the overall model performance.

5. Conclusion

We have used ^{222}Rn to evaluate the simulation of transport in the new planetary multiscale three-dimensional CTM MOCAGE, at resolved as well as at subgrid scales. Two convection schemes (Tiedtke and Kain–Fritsch–Bechtold) and one eddy diffusion (Louis) are used off-line, that is the vertical mass fluxes are computed from the large-scale meteorological variables only.

Results from 1-yr simulations have been used to compare the simulated radon concentrations at different time and space scales, from monthly means to specific episodes, at the surface and at altitude. Several points are noted. First, MOCAGE is able to reproduce the evolution of ^{222}Rn concentration at these different time scales and in the three dimensions; overall results are satisfactory. A conclusion is that the off-line approach as implemented in MOCAGE is valid and compares favourably with on-line simulations, notably by the fact that it is possible to drive simulations with meteorological analyses while in the on-line approach, for the simulation of specific cases, the model has to be nudged towards analyses which can put the physical parametrizations out of balance.

The comparison with 12-hourly observed data is particularly satisfying. On the basis of available observations, tracer transport seems to be well represented in our model. However, some discrepancies remain in some sites, but answers seem to be external to the CTM. In Antarctica, for instance, we advocate that the general bad performance of models could be due to the fact that meteorological conditions near Antarctica are not well represented in the current state-of-the-art, due both to the lack of accurate representation of the extent of sea ice and lack of observations. In Hawaii, we confront an earlier hypothesis that the underprediction of high-altitude radon could be linked to an incorrect specification of the Asian emission source. Second, subgrid transport brings a key contribution to transport, whatever the time scale; simulations without parametrized transport are most of the time particularly bad. The type of convection scheme employed does not seem to have a very sensitive impact on model performances: the two schemes used in the present work behave

quite similarly; indeed, both are of a mass-flux type. Finally, a classification of meteorological conditions leading to high radon in Mace Head (Ireland) has been obtained to interpret the underlying factors. Many points could be tested to improve our results. We have shown that a better resolution allowed, as expected, a better fit to the concentrations. In addition, it is recognized (e.g. Dörr and Münnich, 1990; Dentener et al., 1999) that the emissions depend upon soil types, and the crude assumption of homogeneous 1 atom cm^2 s^{-1} emission rates, however consensual, should be revised.

6. Acknowledgments

Dr Martyn Chipperfield provided the TOMCAT version of Tiedtke's scheme. Dr Peter Bechtold (European Center for Meteorological Weather Forecast) is gratefully acknowledged for the KFB scheme, and helping with its use all throughout this work. Dr Michel Ramonet (Laboratoire des Sciences du Climat et de l'Environnement) kindly provided the radon measurements at Amsterdam Island and Mace Head.

References

Allen, D. J., Rood, R. B., Thompson, A. M. and Hudson, R. D. 1996. Three-dimensional radon 222 calculations using assimilated meteorological data and a convective mixing algorithm. *J. Geophys. Res.* **101**, 6871–6881.

Balkanski, Y. J. and Jacob, D. J. 1990. Transport of continental air to the subantarctic Indian Ocean. *Tellus* **42B**, 62–75.

Bechtold, P., Bazile, E., Guichard, F., Mascart, P. and Richard, E. 2001. A mass flux convection scheme for regional and global models. *Q. J. R. Meteorol. Soc* **127**, 869–886.

Biraud, S., Ciais, P., Ramonet, M., Simmonds, P., Kazan, V., et al. 2000. European greenhouse gas emissions estimated from continuous atmospheric measurements and radon-222 at Mace Head, Ireland. *J. Geophys. Res.* **105**, 1351–1366.

Brost, R. A. and Chatfield, R. B. 1989. Transport of radon in a three-dimensional, subhemispheric model. *J. Geophys. Res.* **94**, 5095–5119.

Cathala, M.-L., Pailleux, J. and Peuch, V.-H. 2003. Improving global chemical simulations of the upper troposphere–lower stratosphere with sequential assimilation of MOZAIC data. *Tellus* **55B**, 1–10.

Chevillard, A., Ciais, P., Karstens, U., Heimann, M., Schmidt, M., et al. 2002. Transport of ^{222}Rn using the regional model REMO: a detailed comparison with measurements over Europe. *Tellus* **54B**, 850–871.

Collins, W.J., Derwent, R. G., Johnson, C. E. and Stevenson, D. S. 2002. A comparison of two schemes for the convective transport of chemical species in a Lagrangian global chemistry model. *Q. J. R. Meteorol. Soc* **128**, 991–1009.

Cros, B., Durand, P., Cachier, H., Drobinski, Ph., Fréjafon, E., et al. 2004. The ESCOMPTE program: an overview. *Atmos. Res.* **69**(3–4), 241–279.

Dentener, F., Feichter, J. and Jeuken, A., 1999. Simulation of the transport of Rn 222 using on-line and off-line global models at different horizontal resolutions: a detailed comparison with measurements. *Tellus* **51B**, 573–602.

Dörr, H. and Münnich, K. O. 1990. ^{222}Rn flux and soil air concentration profiles in West-Germany. Soil ^{222}Rn as tracer for gas transport in the unsaturated soil zone. *Tellus* **42B**, 20–28.

Dufour, A., Amodei, M., Ancellet, G. and Peuch, V.-H. 2004. Observed and modelled "chemical weather" during ESCOMPTE. *Atmos. Res.* in press.

Feichter, J. and Crutzen, P. J. 1990. Parameterization of vertical tracer transport due to deep cumulus convection in a global transport model and its evaluation with ^{222}Radon measurements. *Tellus* **42B**, 100–117.

Genthon, C. and Armengaud, A. 1995. Radon 222 as a comparative tracer of transport and mixing in two general circulation models. *J. Geophys. Res.* **100**, 2849–2866.

Gloersen, P., Campbell, W. J., Cavalieri, D. J., Comiso, J. C., Parkinson, C. L. et al. 1992. *Arctic and Antarctic Sea Ice, 1978–1987: Satellite Passive-microwave Observations and Analysis* NASA publication SP-511. National Aeronautics and Space Administration, Washington, D.C.

International Panel on Climate Change (IPCC) 2001. *Climate Change 2001: The Scientific Basis*. Contribution of Working Group I to the third assessment. Report of the Intergovernmental Panel on Climate Change (IPCC) J. T. Houghton, Y. Ding, D. J. Griggs, M. Noguer, P. J. van de Linden and D. Xiaosi (Eds.) Cambridge University Press, UK, pp 944. *http://www.ipcc.ch/pub/reports.htm*.

Jacob, D. J. and Prather, M. J. 1990. Radon-222 as a test of convective transport in a general circulation model. *Tellus* **42B**, 118–134.

Jacob, D. J., Prather, M. J., Rasch, P. J., Shia, R.-L., Balkanski, Y. J. et al. 1997. Evaluation and intercomparison of global atmospheric transport models using 222 Rn and other short-lived tracers. *J. Geophys. Res.* **102**, 25 931–25 947.

Kain, J. S. and Fritsch, J. M. 1990. A one-dimensional entraining/detraining plume model and its application in convective parameterization. *J. Atmos. Sci.* **47**, 5953–5970.

Kritz, M. A., Le Roulley, J.-C. and Danielsen, E. F. 1990. The China Clipper—fast advective transport of radon-rich air from the Asian boundary layer to the upper troposphere near California. *Tellus* **42B**, 46–61.

Lefèvre, F., Brasseur, G. P., Folkins, I., Smith, A. K. and Simon, P. 1994. Chemistry of the 1991–1992 stratospheric winter: three-dimensional model simulations. *J. Geophys. Res.* **99**, 8183–8195.

Li, Y. and Chang, J. S. 1996. A three dimensional tracer transport model. 1. Evaluation of its transport processes by radon 222 simulations. *J. Geophys. Res.* **101**, 25 931–25 947.

Liu, S. C., McAfee, J. R. and Cicerone, R. J. 1984. Radon 222 and tropospheric vertical transport. *J. Geophys. Res.* **89**, 7291–7297.

Louis, J.-F. 1979. A parametric model of vertical eddy fluxes in the atmosphere. *Bound.-Layer Meteorol.* **17**, 187–202.

Mahowald, N. M., Rasch, P. J. and Prinn, R. G. 1995. Cumulus parameterization in chemical transport models. *J. Geophys. Res.* **102**, 26 173–26 189.

Marenco, A., Thouret, V., Nédélec, P., Smit, H., Helten, M. et al. 1998. Measurements of ozone and water vapour by Airbus in-service aircraft: the MOZAIC airborne program. *J. Geophys. Res.* **103**, 25 631–25 642.

Paatero, J., Hatakka, J., Mattson, R. and Viisanen, Y. 1998. Analysis of daily ^{210}Pb air concentrations in Finland, 1967–1996. *Radiat. Prot. Dosim.* **77**, 191–198.

Polian, G., Lambert, G., Ardouin, B. and Jegou, A. 1986. Long-range transport of continental radon in subantarctic and Antarctic areas. *Tellus* **38B**, 178–189.

Stevenson, S., Collins, W. J., Johnson, C. E. and Derwent, R. G. 1998. Intercomparison and evaluation of atmospheric transport in a Lagrangian model (STOCHEM) and an Eulerian model (UM), using 222 Rn as a short-lived tracer. *Q. J. R. Meteorol. Soc.* **124**, 2477–2491.

Stockwell, Z. and Chipperfield, M. P. 1999. A tropospheric chemical-transport model: Development and validation of the model transport schemes. *Q. J. R. Meteorol. Soc* **125**, 1747–1783.

Tiedtke, M. 1989. A comprehensive mass flux scheme for cumulus parameterization in large-scale models. *Mon. Weather Rev.* **117**, 1779–1800.

Wilkening, M. H. 1959. Daily and annual courses of natural atmospheric radioactivity. *J. Geophys. Res.* **64**, 521–526.

Williamson, D. L. and Rasch, P. J. 1989. Two-dimensional semi-Lagrangian transport with shape-preserving interpolation. *Mon. Weather Rev.* **117**, 102–129.

World Meteorological Organization 1998. *Scientific Assessment of Ozone Depletion, Global Ozone Research and Monitoring Project* WMO Report 44. World Meteorological Organization, Geneva.